

PAPER • OPEN ACCESS

An experimental approach for in-situ characterization of dynamic dissipative properties of road pavements

To cite this article: G Loi *et al* 2024 *IOP Conf. Ser.: Mater. Sci. Eng.* **1306** 012001

View the [article online](#) for updates and enhancements.

You may also like

- [Research on damping performance of elastomer/carbon fiber epoxy composite](#)
Qin Tengfei, Liu Jinsheng, Wei Xing et al.
- [Dynamic mechanical damping analysis of up/step-quenched Cu-Zn-Sn-based shape memory alloys](#)
Justus Uchenna Anaele, Kenneth Kanayo Alaneme and Joseph Ajibade Omotoyinbo
- [Nonlinear Earthquake Response Analysis Using Causal Hysteretic Damping and Extended Rayleigh Damping](#)
Naohiro Nakamura, Kunihiro Nabeshima, Yoshihiro Mogi et al.

PRIME
PACIFIC RIM MEETING
ON ELECTROCHEMICAL
AND SOLID STATE SCIENCE

HONOLULU, HI
October 6-11, 2024

Joint International Meeting of
The Electrochemical Society of Japan (ECSJ)
The Korean Electrochemical Society (KECS)
The Electrochemical Society (ECS)

Early Registration Deadline:
September 3, 2024

MAKE YOUR PLANS NOW!

An experimental approach for in-situ characterization of dynamic dissipative properties of road pavements

G Loi¹, G Marongiu², J Rombi¹, M Coni¹, M C Porcu¹, F Aymerich²

¹ Department of Civil, Environmental Engineering and Architecture, University of Cagliari, Piazza d'Armi, 09123 Cagliari, Italy

² Department of Mechanical, Chemical and Materials Engineering, University of Cagliari, Piazza d'Armi, 09123 Cagliari, Italy

Email address: gabriela.loi@unica.it

Abstract. The dissipative properties of road pavements may have beneficial effects to reduce vehicle vibrations, traffic noise, vehicles-structure dynamic interaction, and degradation of pavement materials. Assessing the dissipative capacity and the damping properties of road pavements is, therefore, of critical importance. Such assessment has been mainly conducted in recent years by laboratory-scale dynamic experiments, while little effort has been devoted to in-situ tests. The latter are, in fact, cumbersome for practical reasons and typically require a more advanced data analysis when highly coupled modes of vibration are involved. Due to the heterogeneity of the road structure, classical methods are not capable of accurately estimating the road damping properties. The present study proposes an alternative experimental approach based on recording signals from accelerometers embedded in the road, which is impacted by an instrumented hammer. The data are analyzed both in the frequency and in the time domains through the combined use of stabilization diagrams and energy decay tools. Multi-mode fitting algorithms are employed to construct stabilization diagrams for the identification of resonance frequencies, while energy decay curves allow for a robust evaluation of the damping values at the identified frequencies. The effectiveness of the approach was assessed on an asphalt road structure.

1. Introduction

High-level vibrations may lead to structural integrity issues, compromising the performance, durability, and reliability of structures. For this reason, energy dissipation under dynamic loads is often valuable in many engineering structures, where dampers are commonly employed to reduce vibrational effects [1]. Examples include earthquake-prone buildings [2], bridges [3], wind turbines [4], rotating machinery [5], and more.

When considering road structures, reducing vibrations may have beneficial effects, including mitigation of pavement material degradation, reduction of traffic noise, better control of vehicle-structure interaction, improved vehicle ride comfort, and minimized transmission of traffic-induced vibrations to adjacent buildings. The influence of the asphalt pavement type on the damping and resonance properties of light-weight bridges was shown in [6], while rubberized asphalt mixtures were suggested as damping layers in roads [7] to reduce detrimental effects on humans and buildings. Assessing the dissipative properties of road pavement structures may be thus of the utmost importance



not only to reduce vibration and noise due to vehicle-road and road-bridge interactions but also to compare the overall performance of different pavement types.

The performance of road pavements has been extensively investigated in the last decades. Deflection methods were proposed to assess the mechanical moduli of road surface and subgrade. To this purpose, Benkelman Beam Deflectometers, lightweight deflectometers [8], and the Falling Weight Deflectometers (FWD) [9, 10] were mainly used. Recording vibrations from sensors bonded to or embedded within the pavement was also exploited to derive performance parameters of road structures under different climate and traffic conditions [11, 12, 13]. Crack propagation and fatigue damage were monitored by means of in situ measures [14] taken through piezoelectric sensors, which are in fact typically used to detect damage in structural components [15].

To account for traffic-induced vibrational effects, the dynamic properties of road systems, like natural frequencies and modal damping ratios, should however be evaluated. The real and imaginary parts of the dynamic complex modulus E^* , which define the elastic and viscous behavior of the material, are often evaluated for linear viscoelastic pavement materials like asphalt mixtures [16]. Guidelines for laboratory tests for measuring E^* values on small unconfined cylindrical specimens are provided by the AASHTO TP 62-07 standard [17]. Based on these tests, the damping properties of different asphalt mixtures were estimated in [16] to quantify the effect on tire/road noise characteristics. Laboratory resonant column tests were also performed to determine the damping properties of rubber-modified asphalt and subgrade soils [18]. Numerical and analytical methods have been proposed for an empirical estimation of the Rayleigh damping matrix from the mass and stiffness matrices when two of the natural frequencies of the system are known [19]. These methods can also be used to assess the influence of subgrade damping on the pavement deflection during simulated FWD tests [20].

In-situ experimental campaigns are better suited than laboratory testing for characterizing the actual dissipative behavior of a road system, as they inherently account for real constraint conditions, pavement material properties, subgrade influences, and interaction phenomena. On the other hand, when non-linear and heterogeneous materials like road pavements and subgrades are involved, assessing modal damping ratios may not be a trivial task and classical methods may prove ineffective, also due to the presence of many heavily coupled modes. An approach to estimate the dissipative properties of pavement and subgrade through in-place tests conducted with a FWD device was proposed in [21]. In this approach the damping ratios were obtained by evaluating the decrease in the peak displacements measured at various distances from the impact given by the FWD. The applied procedure fails however to account for the well-known dependence of damping ratios on the vibration frequencies [22].

The present paper presents an alternative experimental approach to estimate the modal damping ratios of a road system based on impacting the road pavement and recording the signals from accelerometers attached to the pavement. The analysis of the recorded accelerations is carried out in both the frequency and time domains using two different tools: the Stabilization Diagram and the Energy Decay Method. Stabilization Diagrams provide the natural frequencies of the system and an initial estimation of the associated damping ratios. The Energy Decay Method is adopted to directly assess energy dissipation within frequency ranges that include the identified resonance frequencies. The combination of the two tools is expected to lead to a robust and reliable evaluation of the system's damping ratios.

2. In-situ testing set-up

The capability of the proposed approach was assessed on an asphalt road structure consisting of three layers: a subgrade, a granular base layer of 900 mm thickness, and a pavement asphalt layer, the latter composed of binder (80 mm thickness), intermediate (60 mm thickness) and a wearing surface (40 mm thickness).

The road structure was excited utilizing an impact hammer consisting of a steel mass of 9 kg instrumented with an *HBM CFT+ 50kN* piezoelectric force transducer. A rubber pad was interposed

between the hammer and the road pavement to improve the uniformity of the load distribution over the irregular road surface and to control the range of excitation frequencies. A pad thickness of 3 mm was selected after a preliminary series of tests to ensure sufficient energy coverage for frequencies in the range of 0-300 Hz, which are typically associated to traffic loads. Impact forces with peak values of about 45 kN were applied to excite the road structure.

The response of the system was measured with a *Bruel & Kjaer 4370* piezoceramic accelerometer attached to the surface of the road using a thin butyl adhesive tape. The signals of the force and acceleration transducers were fed into *Bruel & Kjaer 2635* charge amplifiers to generate signal voltages, which were finally acquired by a National Instrument *NI9234* PC-controlled data acquisition unit at a sampling rate of 50 kSamples/s.

The inherent heterogeneous microstructure of the material, comprising various constituents (such as aggregates, fillers, and binders) of different shapes and size scales and characterized by the inevitable presence of irregularly distributed voids, cracks, and defects, is expected to lead to a substantial variability in the local dissipative properties of the road pavement. To reduce the effect of local microstructural features and assess the average damping properties over a sufficiently large section of the road structure, a minimum distance of 5 m was chosen between the excitation and the response measurement sites. In addition, to explore how variations in the specific locations of excitation and response acquisition affect the measured damping characteristics, the tests were conducted using three different pairs of input and output locations (testing configurations P1, P2 and P3 in figure 1).

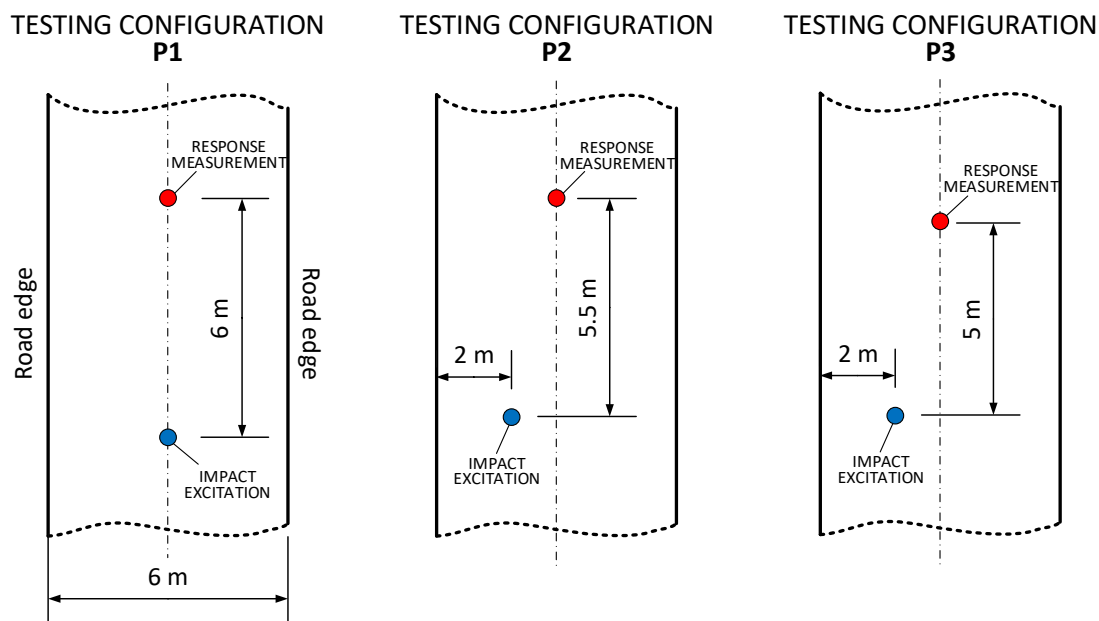


Figure 1. Locations of excitation and measurement points for the three testing configurations.

Figure 2 shows an example of the impact force and the acceleration response signals acquired for the testing configuration P1. The impact force signal has a duration of about 6 ms (figure 2) and a frequency content with a gradually decreasing trend up to approximately 600 Hz (figure 3). As expected, because of the heterogeneity and the wave-dispersive characteristic of the road pavement material, the response signal has a rather complex temporal pattern, characterized by a rapid decay involving multiple damped oscillations with different frequencies. The presence of a multitude of very closely spaced natural frequencies is clear in the frequency spectrum of the measured response, as shown in figure 4. From figure 2, it is immediately evident that the absence of a dominant oscillation with a roughly constant frequency makes it impossible to directly use the basic time-domain approaches (e.g., the Logarithmic Decrement Method) for estimating the damping properties of the system. At the same time, the absence

of well-separated natural frequencies in the response spectrum (see figure 4) hinders the clear identification of contributions from individual modes, thereby impeding the accurate evaluation of damping ratios through conventional frequency-based techniques, such as the Half Power or Circle Fitting methods.

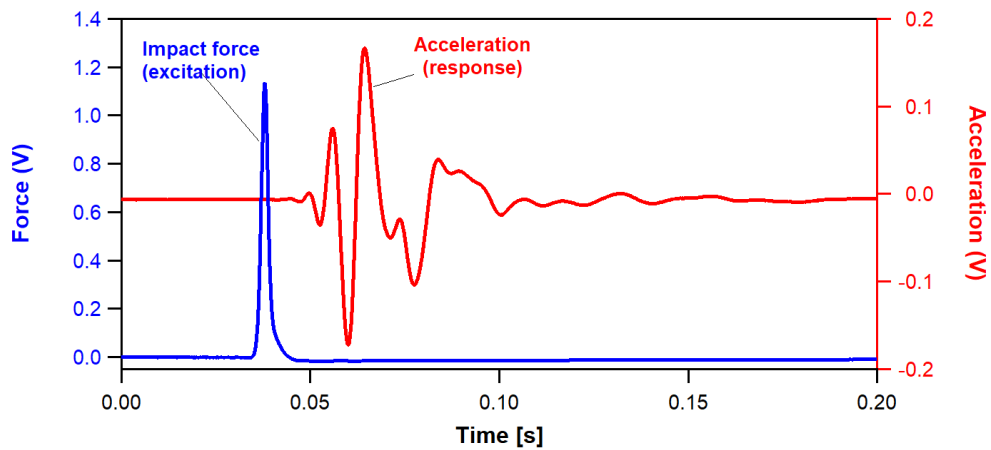


Figure 2. Histories of impact force excitation and acceleration response (testing configuration P1).

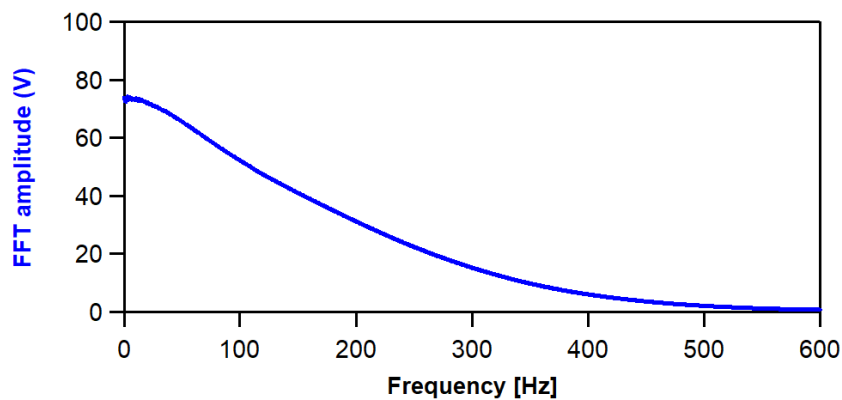


Figure 3. Frequency spectrum of the impact force signal (testing configuration P1).

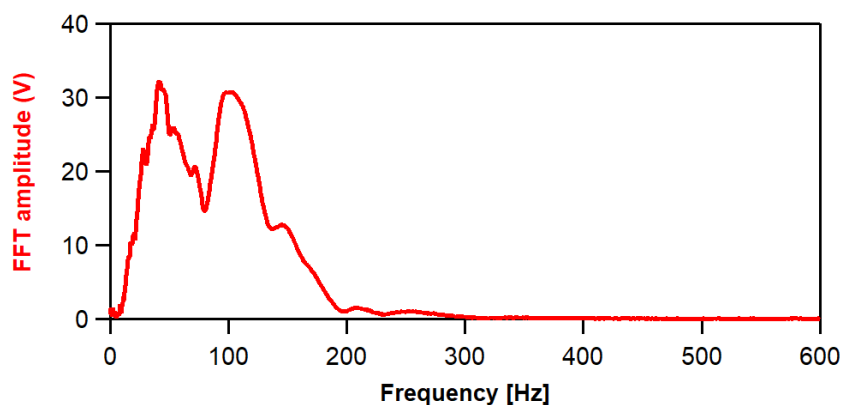


Figure 4. Frequency spectrum of the acceleration response signal (testing configuration P1)

To address these difficulties, a combination of two different techniques is proposed for experimentally determining the damping characteristics of the road pavement. A Stabilization Diagram tool is first applied to identify the natural frequencies of the system and generate a preliminary estimation of the associated damping ratios. An Energy Decay approach, based on the direct assessment of energy dissipation around the identified resonance frequencies, is then employed for a more robust and reliable evaluation of the damping ratios.

3. Results and discussion

Stabilization diagrams provide a concise representation of a system's modal parameters [22], which are extracted through iterative fitting procedures where a modal identification algorithm is repeatedly run by progressively increasing the order of the model (i.e., the number of modes). The main purpose of a stabilization diagram is assessing the accuracy and reliability of a solution, by helping to distinguish between physical modes (which represent the real dynamic response of the system) and spurious modes (generated by noise, overestimation of the model order, or numerical approximations).

The experience gained in many real applications [23] shows that physical modes are stable, i.e., are consistently very close to the same frequency, whereas spurious modes tend to exhibit a wide scatter over a frequency range. In a typical stabilization diagram the information obtained by the identification algorithm over the different model orders is presented with the frequency on the horizontal axis and the model order on the vertical axis. In these diagrams, therefore, physical modes appear as almost straight lines as opposed to spurious modes which tend to scatter over wider frequency ranges.

Figure 5 shows the stabilization diagrams obtained by applying the Direct Modal Parameter Estimation (DMPE) algorithm [24] to the frequency response function (FRF) of the road pavement acquired in the three examined input-output configurations. The criteria adopted to identify physical (i.e., stable) modes require that the difference between the solutions of two consecutive iterations is lower than 1% for the frequency and 5% for the damping ratio [23, 25]. Stable modes are represented as blue markers in the diagrams of figure 5. The data summarized in these charts reveal that the natural modes of the system are distributed in the frequency range 20 Hz–180 Hz. Within this relatively narrow frequency band, the applied algorithm identified several stable poles. In particular, the straight blue lines occurring at 18 Hz, 30 Hz, 46 Hz, 73 Hz, 98 Hz, and 117 Hz identify some of the system's natural frequencies.

It is worth noting that the stabilization diagrams obtained in the three testing configurations do not exhibit significant differences. In particular, the modes identified as stable in both frequency and damping appear to occur at almost the same frequency values, with just slight differences between each testing configuration. The similar responses acquired for the different testing configurations suggests that the size of the examined road portion is large enough to be assumed as representative of the bulk behavior of the road structure.

Stabilization diagrams are conventionally used to distinguish between physical modes and spurious modes, but they do not provide quantitative indications on the damping ratios of the extracted modes. The data condensed in the stabilization diagrams of figure 5 were further post-processed to determine the model order at which the difference between the experimental FRF ($FRF_{ex,i}$) and its estimation based on the extracted modes ($FRF_{num,i}$) is the lower. To assess the optimal model order, the following error function was defined:

$$\varepsilon = \frac{\sum_i (|FRF_{ex,i}| - |FRF_{num,i}|)^2}{\sum_i (|FRF_{ex,i}|)^2}$$

The graphs of figure 6 show the experimental FRFs and their estimation corresponding to the minimum error ε (models with a maximum order of 200 were considered) for the three different input-output configurations.

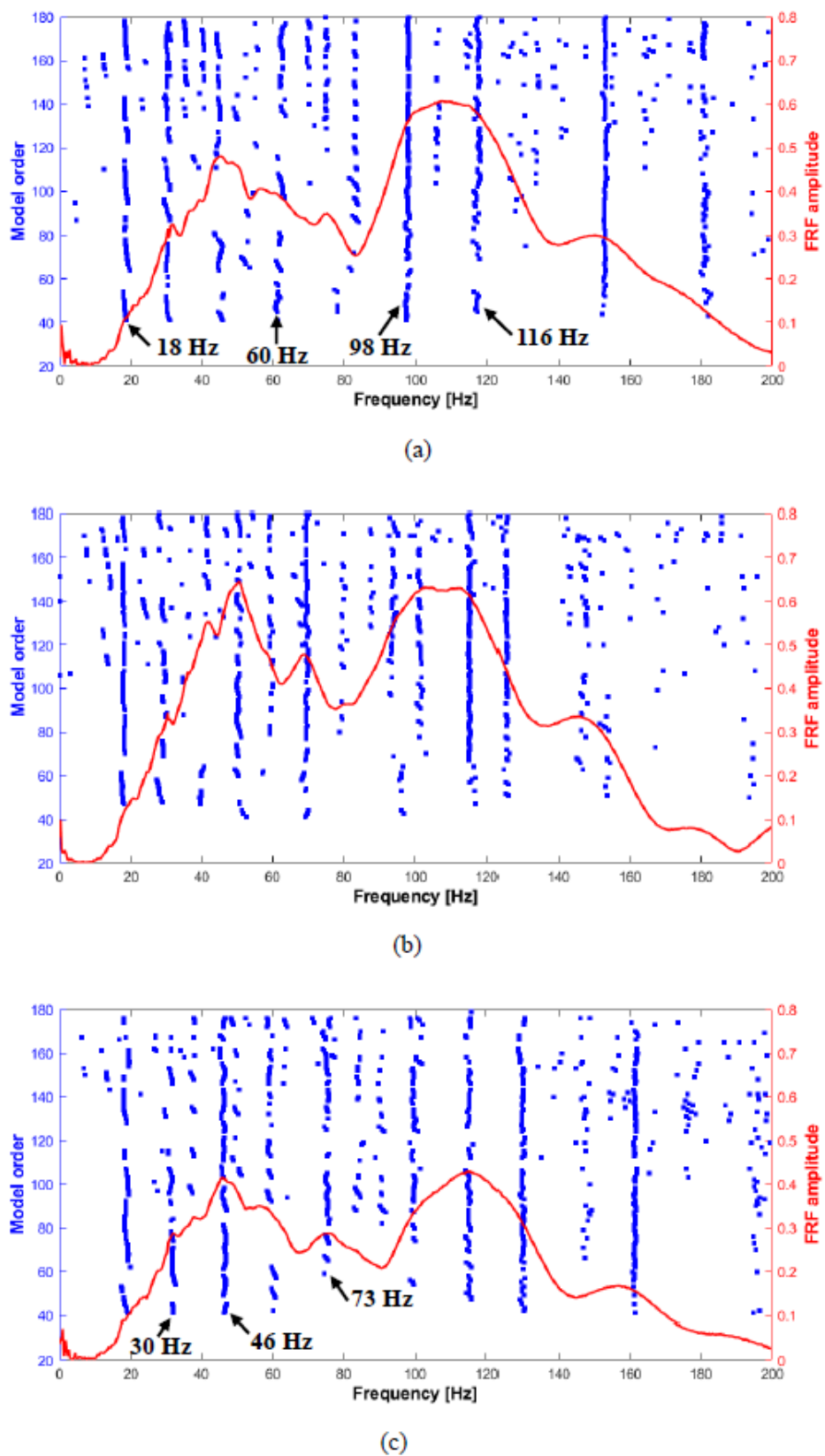


Figure 5. Stabilization diagrams for testing configuration P1 (a), P2 (b), and P3 (c).

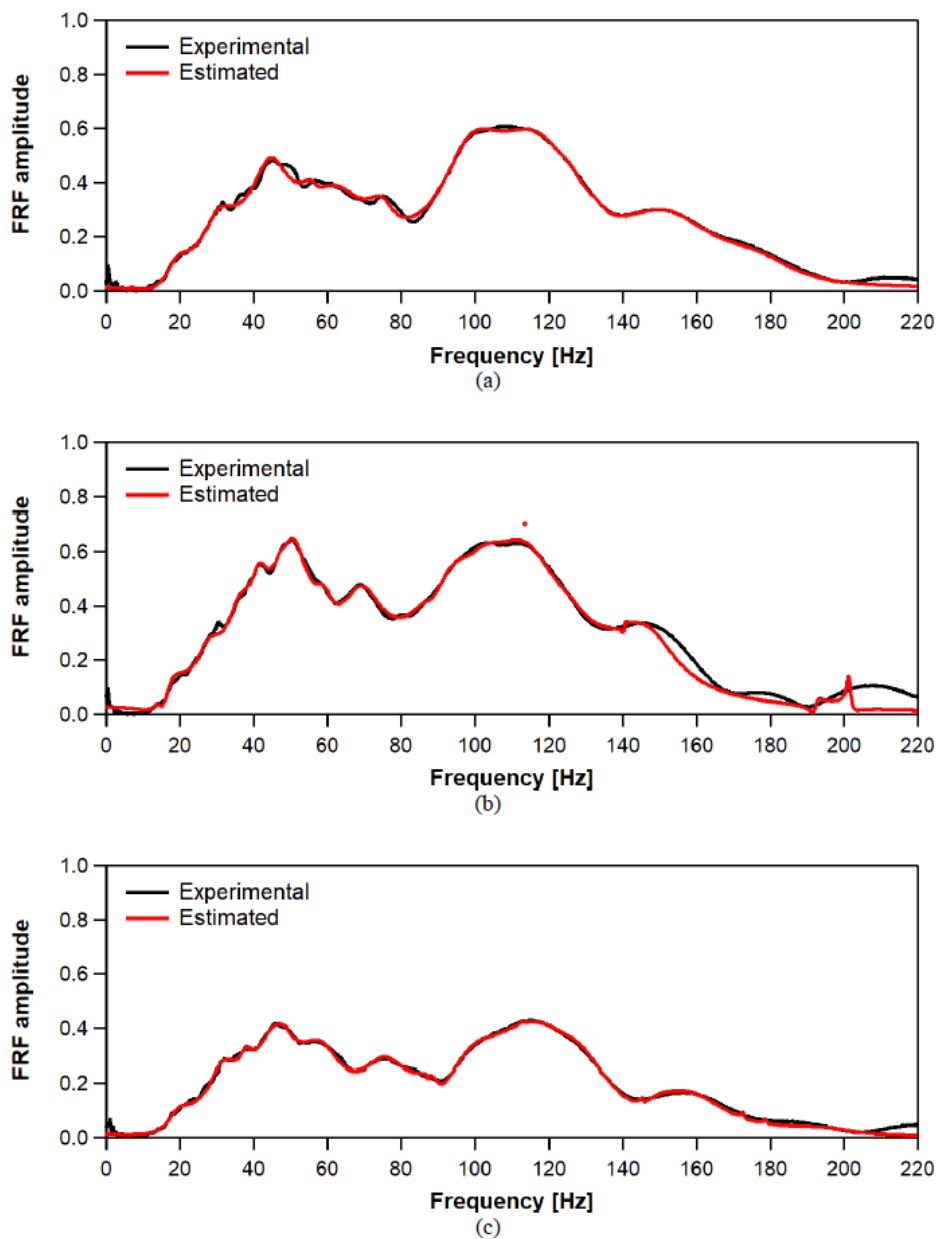


Figure 6. Comparison of experimental and estimated FRFs for testing configuration P1 (a), P2 (b), and P3 (c).

The damping ratios obtained at the optimal model order are reported as a function of the associated resonance frequency in figure 7, for the seven identified stable frequencies. The obtained results show that the damping ratio tends to decrease with increasing frequency. At the lower natural frequencies (i.e., 18 Hz and 30 Hz), the damping ratios range from 13% to 17%, but appear to stabilize around 9% for the 99 Hz and 116 Hz resonances. It can be noticed that for a few natural frequencies the estimated damping ratios exhibit significant dependence on the testing configuration (see for example the values of the damping ratios at the 46 Hz, 60 Hz and 73 Hz frequencies). The high variability of the estimation of the damping characteristics provided by this method for the different input-output locations may be related to both the multi-mode curve-fitting process over a wide frequency range and the presence of many heavily coupled modes.

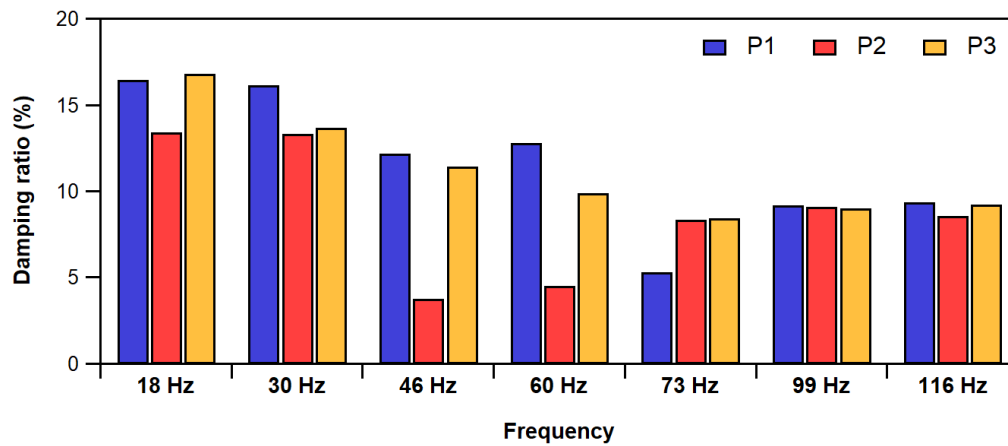


Figure 7. Damping ratios estimated through the Stabilization Diagram tool for the testing configurations P1, P2 and P3.

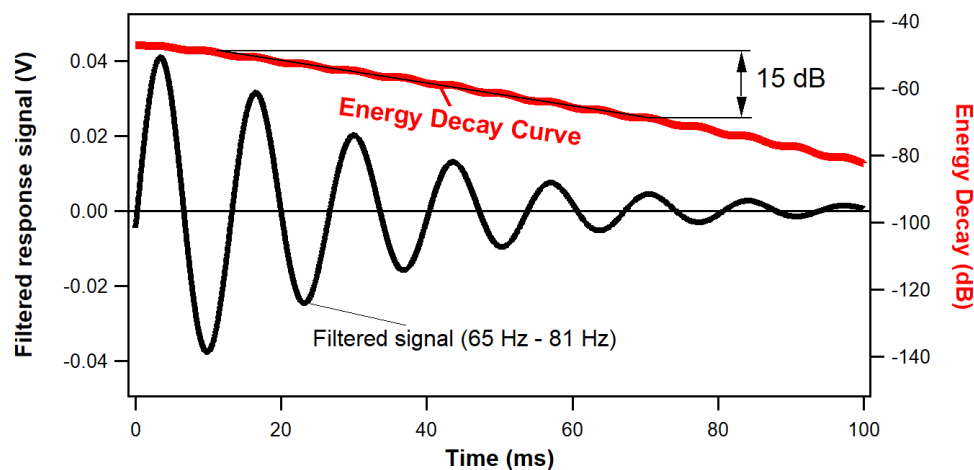


Figure 8. Evaluation of damping ratio using the Energy Decay method

To address this issue, the damping characteristics of the system were subsequently assessed using an Energy Decay approach, based on the evaluation of the decay rate of the time response to an impulse excitation [26, 27]. The analysis was carried out over different frequency bands to account for the dependence of the dissipative properties of the structure on the vibration frequency. The decay rate was evaluated by calculating the slope of a straight line fitted to the energy decay curve of the signal filtered over the investigated frequency band.

The energy decay curve, $E(t)$, was obtained using the backward integration scheme [28] as:

$$E(t) = \int_t^{\infty} h^2(\tau) d\tau$$

where $h(\tau)$ represents the response of the system after pass-band filtering in the frequency range of interest. A band-pass 5th order Butterworth filter with a 1/3 octave bandwidth centered on the desired frequency f_0 was used for filtering the response signal. The energy decay curve was then subjected to linear regression over the range between -2 dB and -17 dB from the maximum level (figure 8). Similar ranges were used in other studies to evaluate the loss ratios of vibrating structures [29, 30]. It is worth

noting that all evaluations carried out on the data acquired in the tests consistently yielded linear regressions with correlation coefficients R^2 higher than 0.98. The slope k of the regression line was then used to calculate the reverberation time (T_{60}) and the damping ratio (ζ) according to the expressions [31]:

$$T_{60} = \frac{60}{k} ; \zeta = \frac{1.1}{T_{60} \cdot f_0}$$

The damping ratios calculated using the energy decay approach for the three testing configurations are presented in figure 9 as a function of the same frequencies examined with the stabilization diagram tool. It is immediately evident that the damping ratios show significantly less variability across the three examined input-output locations when compared to those obtained using the stabilization diagram. The two procedures provide nonetheless globally comparable results when considering the averages of the damping ratios over the three input-output configurations (figure 10). It should be noted that while the energy decay approach appears to be a more reliable and robust approach, it requires prior knowledge of the resonance frequencies of the inspected structure. Because of the inherent heterogeneity and structural complexity of the road structure, this knowledge cannot be easily achieved without the application of multi-mode fitting algorithms, thus suggesting a complementary use of the two approaches for the characterization of the dissipative properties of a road pavement.

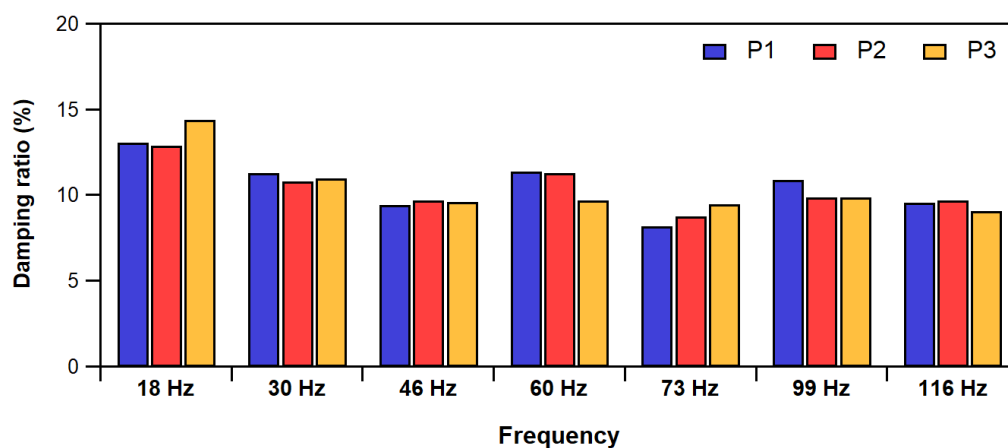


Figure 9. Damping ratios estimated through the Energy Decay approach for the testing configurations P1, P2 and P3.

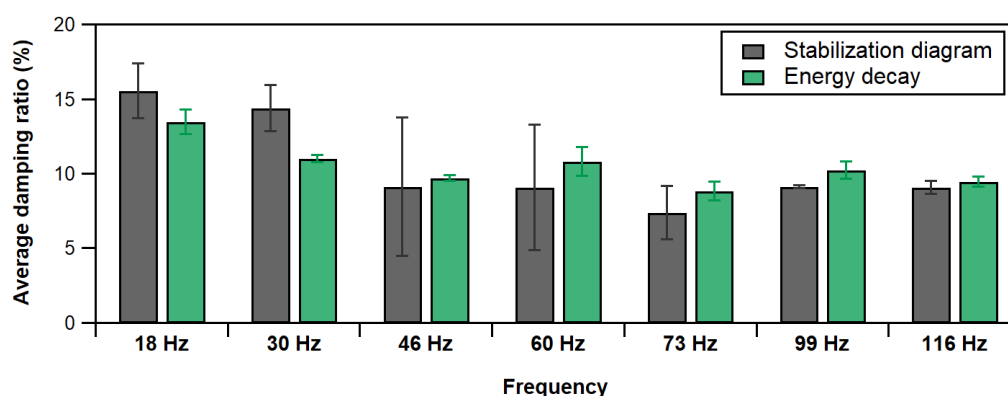


Figure 10. Damping ratios averaged over the three testing configurations: comparison between Stabilization Diagram and Energy Decay approaches.

4. Conclusions

The paper presents an experimental approach to characterize the dissipative properties of a road pavement, relying on signals recorded from accelerometers embedded in the pavement when subjected to instrumented impacts. The main findings of the study can be summarized as follows.

- The impulsive response of the examined road pavement rapidly decays with multiple and heavily coupled vibration modes, preventing the application of classical methods to evaluate damping properties.
- An approach is proposed based on the combined use of stabilization diagrams for the identification of natural frequencies and energy decay measurements for the evaluation of the damping properties of the system within frequency bands around the natural frequencies.
- The construction of the stabilization diagram allows for the identification of natural frequencies by examining the stability of the simulated modes as the model order increases. However, the damping ratios obtained through the stabilization diagram procedure exhibit significant variations across different excitation or measurement locations.
- An energy decay technique is thus subsequently applied to assess the energy dissipation of the system within frequency bands around the natural frequencies identified by the stabilization diagrams. The damping ratios calculated through the energy approach are in reasonable agreement with the average damping ratios obtained over the different testing configurations using the stabilization diagram. The damping ratios obtained using the energy decay method show however a much lower scatter, thus indicating greater reliability and robustness compared to the stabilization diagram tool.
- The potential of the approach will be explored in future work for the assessment of the dissipative properties of different types of engineering structures characterized by complex multi-mode dynamic responses.

References

- [1] Occhiuzzi A 2009 Additional viscous dampers for civil structures: Analysis of design methods based on effective evaluation of modal damping ratios *Eng. Struct.* **31**(5) 1093-101
- [2] Ghiani C, Linul E, Porcu M C, Marsavina L, Movahedi N and Aymerich F 2018 Metal foam-filled tubes as plastic dissipaters in earthquake-resistant steel buildings *IOP Conf. Series: Materials Science and Engineering* **416**(1) 012051
- [3] Wang J F, Lin C C and Chen B L 2003 Vibration suppression for high-speed railway bridges using tuned mass dampers *Int. J. Solid Struct.* **40**(2) 465-91
- [4] Colwell S and Basu B 2009 Tuned liquid column dampers in offshore wind turbines for structural control *Eng. Struct.* **31**(2) 358-68
- [5] Zhao Q, Yuan J, Jiang H, Yao H and Wen B 2021 Vibration control of a rotor system by shear thickening fluid dampers *J. Sound Vib.* **494** 115883
- [6] Schubert S, Gsell D, Steiger R and Feltrin G 2010 Influence of asphalt pavement on damping ratio and resonance frequencies of timber bridges *Eng. Struct.* **32**(10) 3122-29
- [7] Huang J, Leandri P, Cucinello G and Losa M 2022 Mix design and laboratory characterisation of rubberised mixture used as damping layer in pavements *Int. J. Pavement Eng.* **23**(8) 2746-60
- [8] Guzzarlapudi S D, Adigopula V K and Kumar R 2016 Comparative studies of lightweight deflectometer and Benkelman beam deflectometer in low volume roads *Journal of Traffic and Transportation Engineering (English Edition)* **3**(5) 438-47
- [9] Kuo C M, Lin C C, Huang C H and Lai Y C 2016 Issues in simulating falling weight deflectometer test on concrete pavements *KSCE J. Civ. Eng.* **20** 702-8
- [10] Rossi M, Wisén R, Vignoli G and Coni M 2022 Assessment of Distributed Acoustic Sensing (DAS) performance of geotechnical applications *Eng. Geol.* **306** 1-14
- [11] Čygas D, Laurinavičius A, Paliukaitė M, Motiejūnas A, Žiliūtė L and Vaitkus A 2015 Monitoring

- the mechanical and structural behavior of the pavement structure using electronic sensors *Comput.-Aided Civ. Infrastruct. Eng.* **30** 317-28
- [12] Bahrani N, Blanc J, Horny P and Menant F 2020 Alternate method of pavement assessment using geophones and accelerometers for measuring the pavement response *Infrastructures* **5**(3) 25
- [13] Coni M, Mistretta F, Stochino F, Rimbi J, Sassu M and Puppio M L 2021 Fast Falling Weight Deflectometer method for condition assessment of RC bridges *Appl. Sci.* **11** 1-18
- [14] Alavi A H, Hasni H, Lajnef N and Chatti K 2016 Continuous health monitoring of pavement systems using smart sensing technology *Constr. Build. Mater.* **114** 710-36
- [15] Loi G, Marongiu G, Porcu M C and Aymerich F 2023 Vibro-Acoustic Modulation with broadband pump excitation for efficient impact damage detection in composite materials *IOP Conf. Series: Materials Science and Engineering* **1275**(1) 012008
- [16] Biligiri K P 2013 Effect of pavement materials' damping properties on tyre/road noise characteristics *Constr. Build. Mater.* **49** 223-32
- [17] AASHTO 2006 Designation: TP 62-07, Determining dynamic modulus of hot-mix asphalt concrete mixtures. AASHTO Provisional Standards
- [18] Zhong X G, Zeng X and Rose J G 2002 Shear modulus and damping ratio of rubber-modified asphalt mixes and unsaturated subgrade soils. *J. Mater. Civ. Eng.* **14**(6) 496-502
- [19] Huang J, Li X, Zhang J, Sun, Y and Ren J 2022 Determining the Rayleigh damping parameters of flexible pavements for finite element modeling *J. Vib. Control* **28**(21-22) 3181-94
- [20] Kuo C M and Tsai T Y 2014 Significance of subgrade damping on structural evaluation of pavements *Road Mater. Pavement Des.* **15**(2) 455-64
- [21] Uglova E and Tiraturyan A 2017 Calculation of the damping factors of the flexible pavement structure courses according to the in-place testing data *Procedia Eng.* **187** 742-8
- [22] Avitabile P 2018 *Modal testing – A practitioner's guide* (Chichester: John Wiley & Sons Ltd) p 544
- [23] Van der Auweraer H and Peeters B 2004 Discriminating physical poles from mathematical poles in high order systems: use and automation of the stabilization diagram *Proceedings of the 21st IMTC 2004 - Instrumentation and Measurement Technology Conference* (IEEE Cat. No. 04CH37510) 2193-8
- [24] Chomette B and Mamou-Mani 2017 Modal control based on direct modal parameters estimation *J Vib. Control* **24**(12) 2389-99
- [25] Wu C, Liu H, Qin X and Wang J 2017 Stabilization diagrams to distinguish physical modes and spurious modes for structural parameter identification *J. Vib. Eng.* **19**(4) 2777-94
- [26] Cremer L, Heckl M and Petersson B A T. *Structure-Borne Sound - Structural Vibrations and Sound Radiation at Audio Frequencies* (Berlin: Springer Verlag) p 607
- [27] Bloss B and Rao M D 2005 Estimation of frequency-averaged loss factors by the power injection and the impulse response decay methods *J. Acoust. Soc. Am.* **117**(1) 240-9
- [28] Schroeder M R 1965 New method of measuring reverberation time *J. Acoust. Soc. Am.* **37**(6) 1187-8
- [29] Cabell R, Schiller N, Allen A and Moeller M 2009 Loss factor estimation using the impulse response decay method on a stiffened structure *Proceedings Inter-noise 2009 - 38th International Congress and Exposition on Noise Control Engineering*
- [30] Wu L, Agren A and Sundbäck U 1997 A study of the initial decay rate of two-dimensional vibrating structures in relation to estimates of loss factor *J. Sound Vib.* **206**(5) 663-84
- [31] Gade S and Herlufsen H 1994 Digital filter techniques vs FFT techniques for damping measurements *Brüel & Kjaer Technical Review* **1** 1-44.